A Computational and Experimental Investigation into Mechanical Characterizations of Strut-Based Lattice Structures

Mohammad Reza Vaziri Sereshk[1,2], Kevin Triplett[1,2], Christopher St. John[1], Keith Martin[1], Shira Gorin[1], Alec Avery[1], Eric Byer[1], Conner St Pierre[1], Arash Soltani-Tehrani[1,2], Nima Shamsaei[1,2*]

[1]Department of Mechanical Engineering, Auburn University, Auburn, AL

[2]National Center for Additive Manufacturing Excellence (NCAME), Auburn University, Auburn, AL

[*]Corresponding author:

Email: shamsaei@auburn.edu

Phone: (334) 844-4839

Abstract

Strut-based lattices are widely used in structural components for reducing weight. Additive manufacturing has provided a unique opportunity to fabricate such complex geometries. In addition to the unit cell type, the strut size and shape can significantly affect the mechanical properties achieved. Therefore, furnishing a lattice structure library may help in selecting the appropriate combination of lattice types and dimensions for targeted mechanical performance for a specific application. This study presents a method for determination of mechanical properties, including strength and stiffness, for lattice structures. Finite element (FE) simulations are used as the main tool and the results of which are to be verified by mechanical testing of samples fabricated using the laser beam powder bed fusion (LB-PBF) process. Proper lattices with the stiffness matched with associated bone were determined. However, the result indicated that lattices made from 316L SS are not strong enough for bone implants. The proposed procedure can be used for other unit cells of interest due to its generality.

Introduction

In order to create biomedical implants that do not have negative effects on the surrounding bone, an alternative with a similar modulus of elasticity to bone is required [1-5]. The target values for the modulus of elasticity are nearly a tenth of the value for the titanium alloys commonly used in biomedical implants. While current implants are most often solid structures, modern research has investigated using lattice structures to reduce the stiffness of implants [2, 6, 7]. To create a structure that approaches the desired modulus of elasticity, a density gradient is usually applied to the final structure [8]. Ultimately, the core of the structure is denser than the outer structure [8, 9]. This gradient change is discussed by Xu-bin et al [10]. Bio-medical implant data is available in Ref. [11] which is widely-used data source for design of lattices. Shrestha et al. [12] studied the behavior of lattices under tensile loading; however, determination of behavior in compression is crucial for bio-medical implant applications.

The work that follows is the preliminary process examining the stress effects of changing volume fraction. This is critical for choosing the most promising lattices as well as determining

which parameter is most consequential to change regarding the stress profiles of the lattices. Throughout the design and analysis process, a library of the seven lattices was compiled. This library serves as a reference for the research and contains mechanical properties of each lattice's varied volume fraction. This will assist in deciding which lattice structures exhibit the preferred mechanical properties. Once the data is acquired, it will be used in conjunction with other biomechanical data, to assist in the creation of a patient specific implement that reduces the surgery's complications as well as improving life after the implant.

Architectural Design Development

To obtain adequate research data, the authors selected seven different unit cells to analyze (see Table 1). All strut-based unit cells analyzed were variants of face centered cubic (FCC) and body centered cubic (BCC) unit cells. They were chosen because of applicability in biomedical implants and manufacturability by additive manufacturing processes.

Varying volume fraction allows for a variation in porosity and relative density of the unit cell structure. Increasing porosity promotes decreased weight and stiffness of the structure. This is desirable because the implant will more closely mimic the stiffness of the bone that it will be integrated with, reducing the effect of stress shielding. Additionally, a lattice structure promotes a higher degree of osseointegration between bone and implant than a solid material because it contains space in which bone tissue can grow.

SolidWorks is the software used for modeling and simulation. The process of computer aided design (CAD) file generation for lattice samples started by creating a unit cube, with equal dimensions on the x, y, and z axes and centered at the origin. Construction planes were then created at appropriate orientations from which struts could be extruded to form the unit cell. All dimensional parameters were linked together, lengths based off cubic width and diameters made equal to the first strut extruded. This linkage allows the user to modify parameters of a completed lattice structure by changing just two dimensions. From this point, construction direction lines in x, y, and z axes were created. The linear pattern and mirror features were used to produce a 6x6x6 unit cell lattice structure in those directions. Table 2 illustrates the different lattice structures, and Table 3 shows the varying dimensions of a BCCZ lattice structure. All lattices were initially tested at strut diameters of 0.4, 0.8, 1, 1.5, and 2 mm.

Table 1: Unit Cells
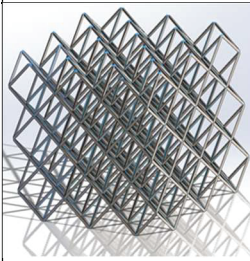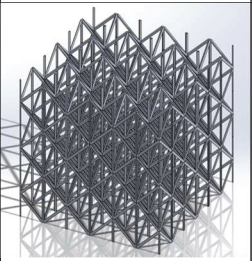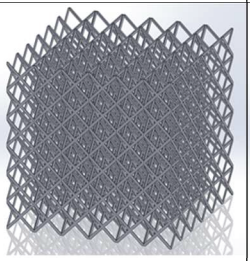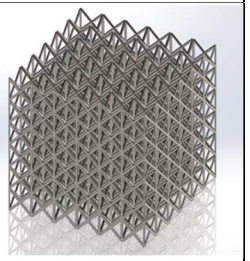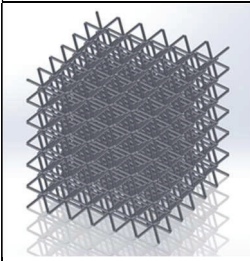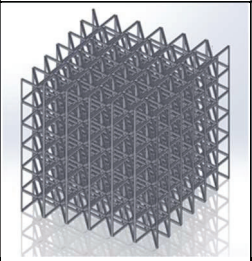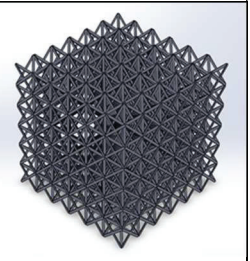
FCC	FCCZ	F2CC	F2CCZ
BCC	BCCZ	F2BBC	

Table 2: Lattice samples

FCC	FCCZ	F2CC	F2CCZ
BCC	BCCZ	F2BCC	

In this step of the study, stainless steel 316L SS was selected for all FEA analysis for the sake of cost effectiveness. Applicability of this type of bio-compatible metal for this purpose will be discussed later but was selected based on the work done by Chen et al. [13]. Associated material properties needed for the simulation was available by default in SolidWorks.

Computing Issues/Mesh Adequacy

Since this study was heavily based on finite element analysis, ensuring the accuracy of the simulation results is pivotal. An analysis of meshes of different elements sizes was performed to converge to an appropriate mesh. Due to time constraints, an optimally coarse mesh had to be used to save simulation time. The complexity of these 6x6x6 lattice structures caused meshing issues as well.

In order to prove the accuracy of the mesh that was selected, a beam structure fixed at both ends was simulated. It was loaded with a single point load at the center and the max stresses and displacements were compared to traditional hand calculations of a beam loaded under the same conditions. Mechanics of materials equations (Eqs. (1) and (2)) were used to calculate stress and displacement of this type.

Maximum moment: $\sigma = \frac{My}{I}$ (1)

Maximum displacement: $\Delta = \frac{Pl^3}{192EI}$ (2)

The analyzed model is shown in Figure 1(a). The analysis was based on a beam of 10 mm in length and 1 mm in diameter to closely simulate a lattice strut. Identical simulations were run on a variety of meshes until there was a convergence in the stress value. As shown in Figure 1(b), even a mesh with twenty times more elements displayed similar results to the coarser meshes. The values still have a slight variation of approximately 5% with respect to the hand calculations

because the nodes of the mesh were not in the exact same location each time the comparison values were taken [14].
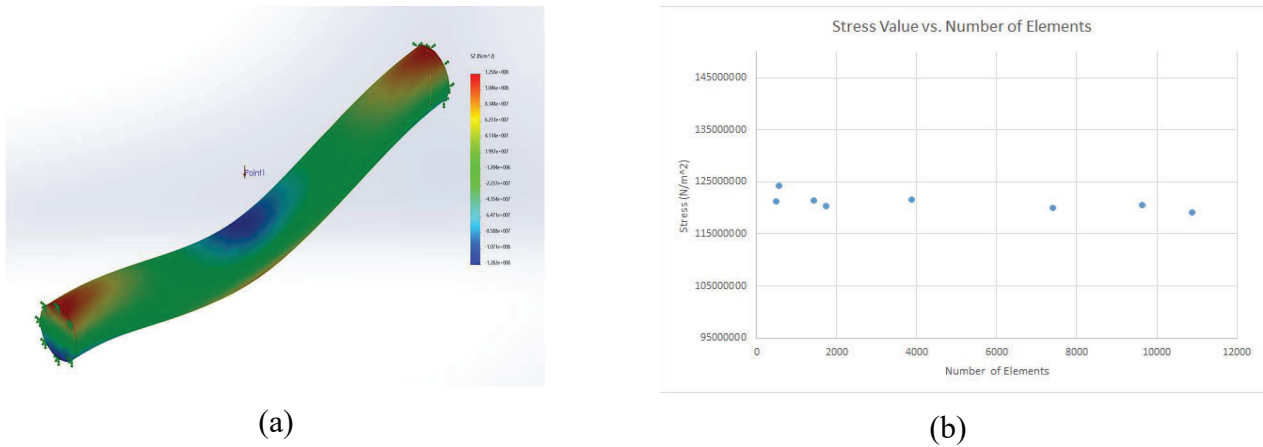

(a)

(b)

Fig. 1. Mesh adequacy evaluation; (a) 3D model of beam, (b) numerical convergence of FE solution

Parameter Dependency Study

Volume fraction defined by relative density of the lattice structures to a solid cube of wrought stainless steel is examined as the main parameter. Various lattice 6*6*6 samples with different sizes but identical volume fractions were constructed for each unit cell (see Table 3 for an illustration of proportional differences and Table 4 for lattice properties). The provided data confirms that the given unit cell lengths and strut diameters produce equal mass and volume fractions. Further FEA was performed to confirm that volume fraction is the only parameter that influences Elastic Modulus.

Table 3: BCCZ Lattice Variations

.4 mm	.8 mm	1 mm	1.5 mm	2 mm

The design studies were created by fixing a central node on the bottom of the lattice, then applying a roller/slider constraint on the rest of the bottom nodes. Roller/slider constraints were used instead of fixed geometry to avoid unnecessary and inaccurate moments being applied to bottom nodes. The top nodes were subjected to homogeneous prescribed displacement, which was increased incrementally in consecutive studies until the resulting stress reached yield for the material. The same process was repeated across all unit cells and all volume fractions. Properties

were then compared to those of wrought material and effective values for the lattices were extrapolated.

Table 4: Mass and Volume Fraction Calculations

Unit Cell Length (mm)	Strut Diameter (mm)	Cube Mass (g)	Lattice Mass (g)	Mass Fraction	Cube Volume (mm^3)	Lattice Volume (mm^3)	Volume Fraction
5	1	216.73	35.9	0.16564	27000	4472.06	0.165631
10	2	1733.83	287.19	0.16563	216000	35777.87	0.165638
15	3	5851.68	969.27	0.16563	729000	120751.19	0.165639
20	4	13870.6	2297.52	0.16563	1728000	286223.88	0.165638

The visual displacement results for this process can be found in Figure 3, while Figure 4 shows the Von Mises stress contour. As expected, the boundary conditions imposed on the models resulted in homogeneous distributions of displacement, and symmetric distributions of stress. It is important to note that maximum stress locations, colored red on the stress map, are found where the geometry changes abruptly due to stress concentration at strut intersection. These stress concentrations, or hotspots, are to be expected. The few outliers in the data collected generally were caused by hotspots behaving asymmetrically. Fortunately, these outliers can generally be ignored due to the ability to correlate data with lattices using different volume fraction parameters. In further FEA studies, these hotspots can be mitigated by changing geometry such that strut intersections occur more smoothly. Table 5 summarizes the result for parameter dependency study.

The data in Table 5 demonstrates that the effective elastic modulus remains constant, within ± 0.84%, when unit cell length and strut diameter parameters are changed while keeping volume fraction equal. This further proves that volume fraction is the only parameter that effects lattice strength.
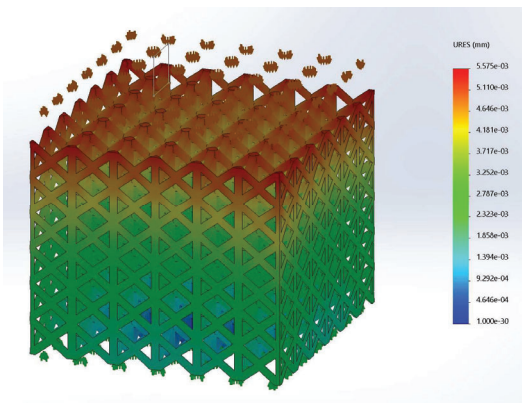

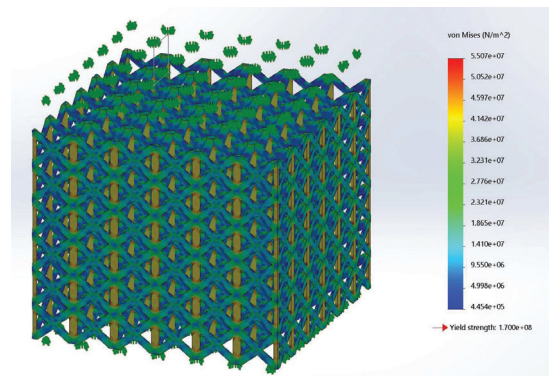Figure 1: F2CCZ Displacement Study

Figure 2: F2CCZ Von Mises Study

Table 5: Effective Elastic Modulus calculation

Unit Cell Length (mm)	Strut Diameter (mm)	Area (mm^2)	Force (N)	Effective Stress (MPa)	ΔL (mm*E-03)	L (mm)	Strain (*E-5)	Effective Elastic Modulus (N/m^2*E+10)
5	1	900	1728	1.92	5.00	30	16.7	1.15
10	2	3600	3485.3	96.8	5.00	60	8.33	1.16
15	3	8100	5211.2	64.3	5.00	90	5.56	1.16
20	4	14400	6939.5	48.2	5.00	120	4.17	1.16

Max:	1.16E+10
Min:	1.15E+10
%Diff:	8.48E-01

Based on the procedure discussed in next section, stiffness and yield strength of lattice samples were determined. Specific strength was also calculated and included in addition to the previous values.

Parameter Dependency of Mechanical Properties

Through the described finite element method, the effect of volume fraction on the mechanical properties of all seven unit cell lattice variations was investigated. The properties analyzed were effective elastic modulus, effective yield strength, and specific strength (strength-to-weight ratio). After performing many iterations of the described method applying different loads the force versus displacement curve (an example in Fig. 5) is obtained. Then apparent stress and strain are calculated and Elastic Modulus is determined as the slope of stress-strain line. Yield stress is also considered as the apparent stress at onset of exceeding maximum Misses stress of the structure from yield strength of 316L SS. If the structure meets this condition, it begins to deform permanently. As an example, the force versus displacement diagram for the BCC lattice structure with a 1.06 mm diameter is presented in Figure 5. Figures 6 to 8 summarize the data generated as the library of unit cells which contains variation of stiffness and strength with volume fraction for each type of cells.

By generating this data and understanding these relationships, the bio-implant designers can optimize specific mechanical properties based on the application of the product being designed. If a design requirement is weight, stiffness, strength, or some combination of all, they have the capability with this study and method to vary volume fraction (unit cell geometry and type) in a particular part and achieve desired properties in all locations of the product.
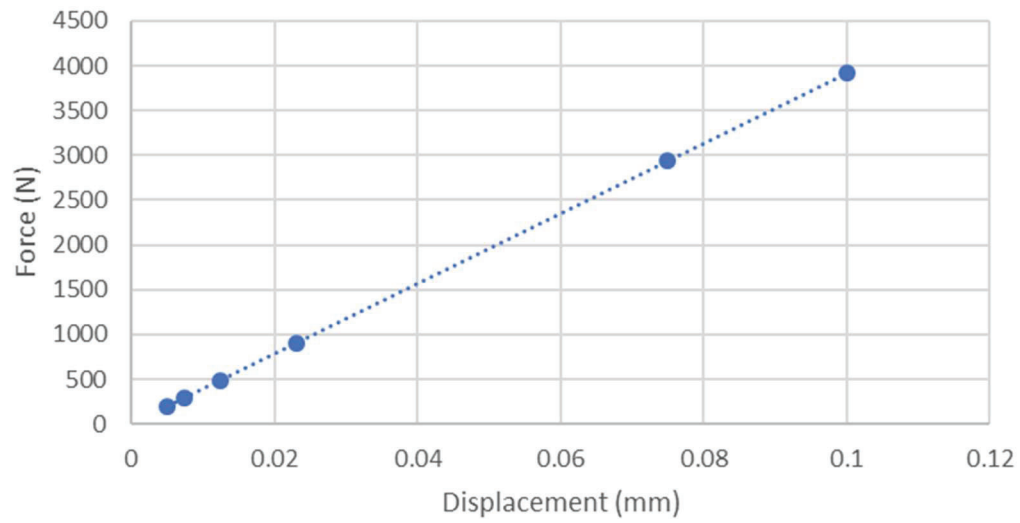
Figure 5: BCC 1.07 mm Diameter, Force – Displacement variation
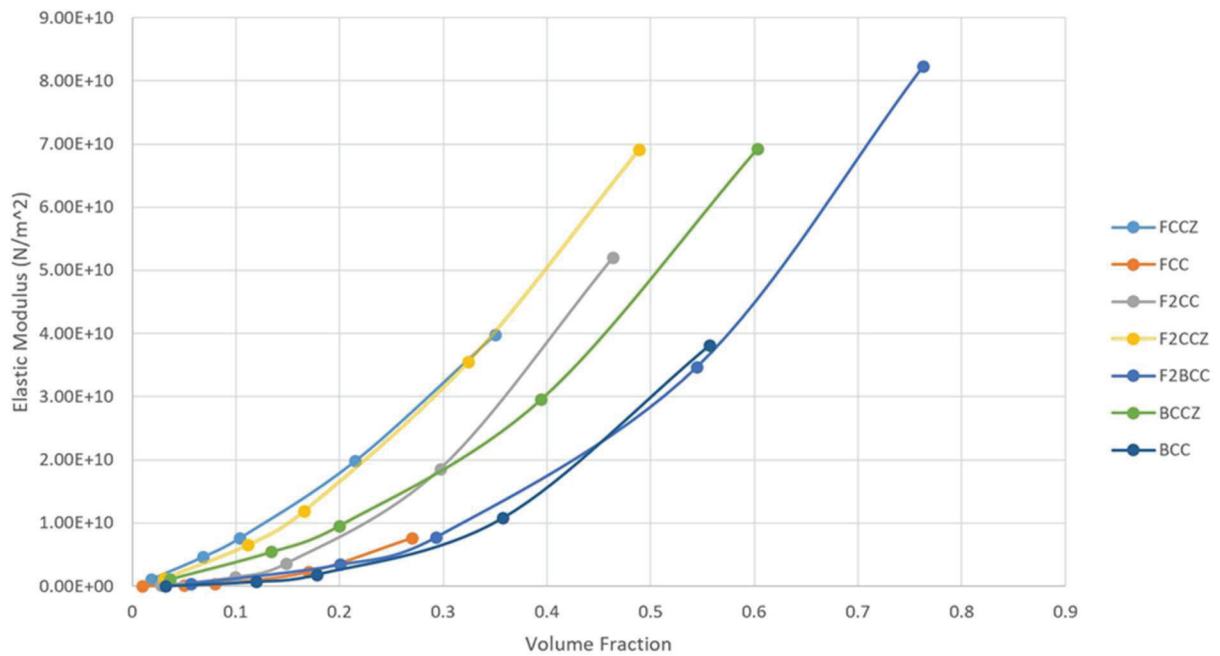
Figure 6: Variation of Elastic Modulus with volume fraction
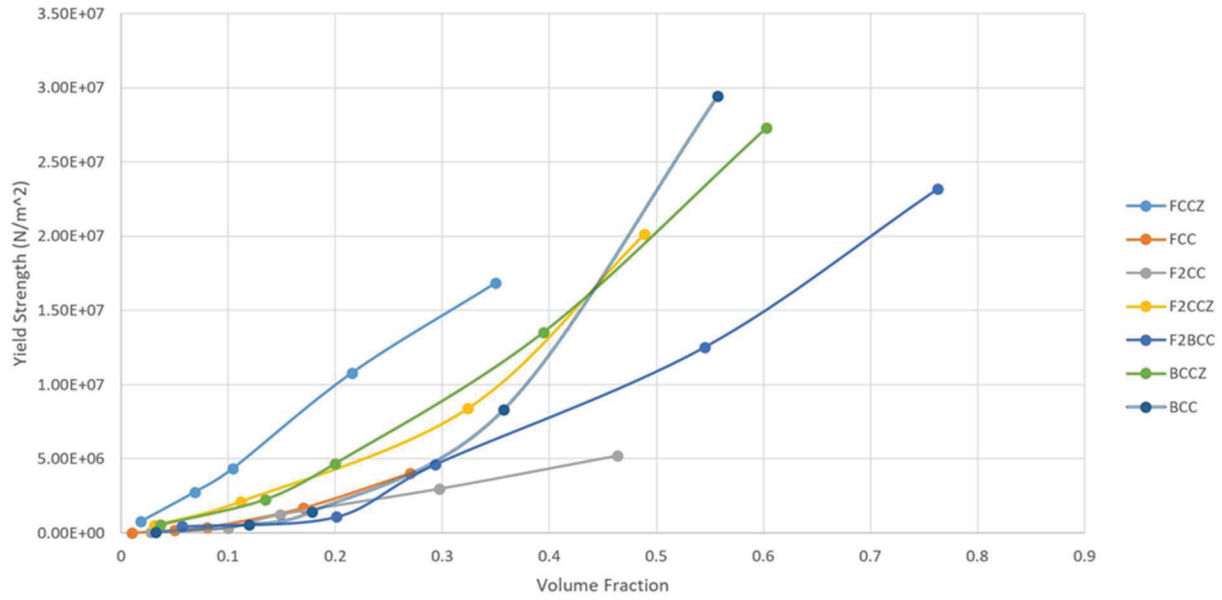
Figure 7: Yield Strength Comparison
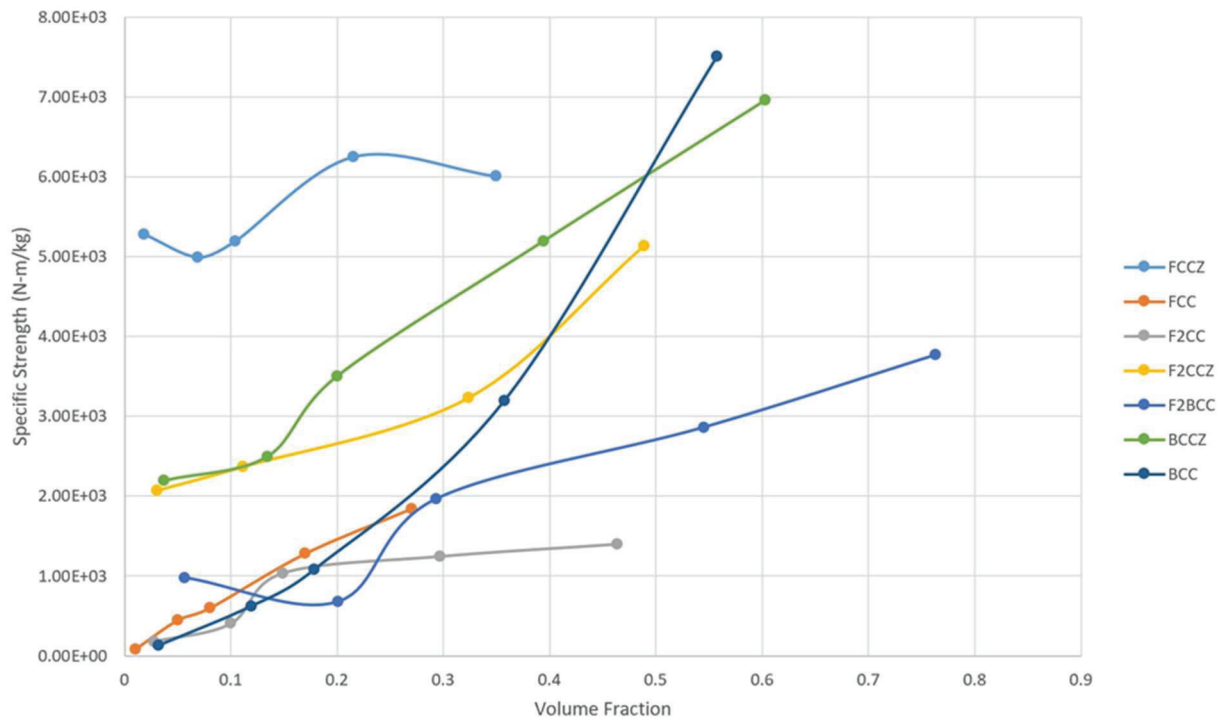
Figure 8: Specific Strength Comparison

Practical Application of Lattice Library

Referring to the data provided by Zhang, et al. [5] for human bones, it was attempted to find proper lattices as the replacement for bones with the application in bio-implants. The proper volume fractions for each unit cell are defined by matching stiffness from Ref. [5] with associated ones in

our library of lattices (Fig. 6). The corresponding unit cell volume fractions are shown in Table 6. The dimension or size of the cells can be determined in further step of design.

Table 6: Data for the lattices for the application in bone implants

Bone	Age/Gender (average)	Elastic Modulus of Bone (Gpa)	Volume Fraction						
			FCC	FCCZ	F2CC	F2CCZ	BCC	BCCZ	F2BCC
Fibula	33 male	19.2	0.3854	0.1946	0.3093	0.2309	0.4503	0.3228	0.4435
	59 female	15.2	0.3548	0.1643	0.2794	0.1992	0.4146	0.2800	0.4022
Humerus	15-89 male	15.6	0.3581	0.1674	0.2826	0.2025	0.4185	0.2846	0.4067
	15-89 female	16.1	0.3621	0.1713	0.2865	0.2066	0.4232	0.2902	0.4121
Tibia	20-89 male	25	0.4228	0.2344	0.3471	0.2722	0.4939	0.3762	0.4944
Femur	20-89 female	17	0.3692	0.1783	0.2933	0.2138	0.4314	0.3000	0.4216

Although it was possible to find proper unit cells for each application based on matching stiffness, the strength of the selected lattices is far below the corresponding bone (in order of 100 MPa [5]). Considering the higher strength of lattices in tension (3-5 time larger), they are still significantly weak for this application (see Fig. 7). The proposed solution is changing material from 316L SS to Ti6Al4V which is widely-used standard material for biomedical implants, referring to Ref. [15].

Experiment

Computer aided manufacturing (CAM) files were generated at National Center for Additive Manufacturing Excellence (NCAME) for all seven lattices using Materialise Magics software and then sent to EOS 290 metal 3D printer to fabricate samples for testing. Due to some manufacturability issues Ti64 is considered for printing the samples and those simulations used for evaluation of FE models are to be repeated with appropriate material data, consequently. Figure 9 shows some of the fabricated lattice compression samples and Figure 10 indicates the compression test setup.
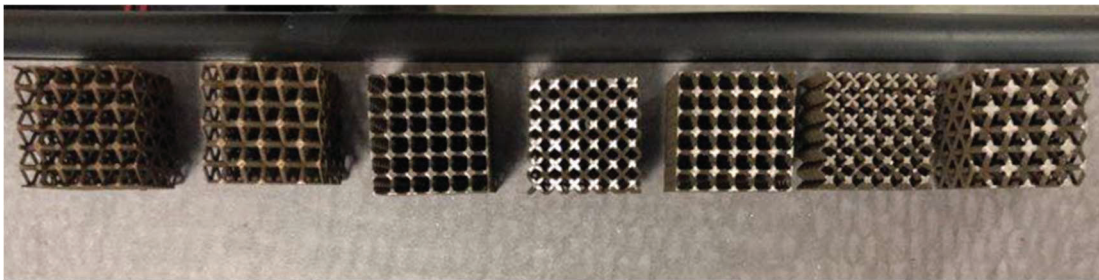

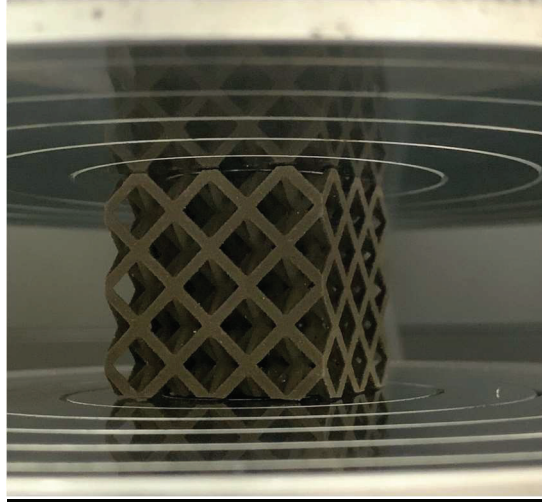Fig. 9. Lattice compression samples designed and manufactured in NCAME

Fig. 10. Setup for compression test

Tables 7 and 8 summarize the result obtained from two tests for Elastic Modulus and maximum force. Maximum force is considered as the force which creates plastic deformation in structure.

Table 7: Measured Elastic Modulus in experiments

Elastic Modulus Test Results						
	BCC	BCCZ	FCC	FCCZ	F2CCZ	F2CC
Test 1 (GPa)	0.4	0.906	0.71	1.11	1.43	1.06
Test 2 (GPa)	0.4	N/A	0.71	1.16	1.58	1.16
% Difference	0.00%	N/A	0.71%	4.50%	10.49%	9.43%

Table 8: Measured maximum forces in experiments

Maximum Force Test Results						
	BCC	BCCZ	FCC	FCCZ	F2CCZ	F2CC
Test 1 (kN)	19.72	39.9	30.65	61.33	68.8	46.92
Test 2 (kN)	20.66	N/A	31.51	61.31	67.99	47.96
% Difference	4.55%	N/A	2.73%	0.03%	1.19%	2.17%

As it can be seen in Tables 7 and 8, the results obtained for two tests are in a good agreement and repeatability of experiment is guaranteed. These data will be used for evaluation purposes in the next step of this comprehensive study.

Conclusion

The research-based approach of studying these lattice structures lead the authors to investigate the effect of volume fraction on elastic modulus, yield strength, and specific strength. This was done because the volume fraction study that was performed indicated that the main factor affecting these mechanical properties is volume fraction and not individual dimensions. These issues caused limitations to the mesh capabilities for the simulations, so an in-depth mesh analysis was performed to ensure that coarser meshes presented similar results to finer meshes.

At its current state, the project has generalized a design optimization method by utilizing the relationships between mechanical properties and the geometries of a particular lattice structure. The process provides designers with the ability to vary structures with volume fraction to achieve desired properties in specific locations of a product. In practical application, the stiffness can be matched and proper lattices can be determined as the replacement of different human bones in bio-medical implants. However, there is an issue with matching strength. Selected lattice structures made from 316L SS are significantly weaker than associated bones. Therefore, Ti6Al4V with higher strength and lower density would be used to fabricate lattices in further steps of this study.

References

1. Balla, Vamsi Krishna, et al. "Porous Tantalum Structures for Bone Implants: Fabrication, Mechanical and In Vitro Biological Properties." *Acta Bomaterialia*, vol. 6, no. 8, Aug. 2010, pp. 3349-59, doi:10.1016/j.actbio.2010.01.046. Accessed 26 Feb. 2019.

2. He, Yuhao, et al. "Solid-Lattice Hip Prosthesis Design: Applying Topology and Lattice Optimization to Reduce Stress Shielding from Hip Implants." *Proceedings of the Design of Medical Devices Conference*, pp. 1-5, doi:10.1115/DMD2018-6804. Accessed 28 Feb. 2019.

3. Rahimizadeh, Amirmohammad, et al. "Porous Architected Biomaterial for a Tibial-Knee Implant with Minimum Bone Resorption and Bone-Implant Interface Micromotion." *Journal of the Mechanical Behavior of Biomedical Materials*, vol. 78, Feb. 2018, pp. 465-79, doi:10.1016/j.jmbbm.2017.11.041. Accessed 25 Feb. 2019.

4. Wang, Xiaojian, et al. "Topological Design and Additive Manufacturing of Porous Metals for Bone Scaffolds and Orthopaedic Implants: A Review." *Biomaterials*, vol. 83, Mar. 2016, pp. 127-41, doi:10.1016/j.biomaterials.2016.01.012. Accessed 26 Feb. 2019.

5. Zhang, X. Z., et al. "Selective Electron Beam Manufactured Ti-6Al-4V Lattice Structures for Orthopedic Implant Applications: Current Status and Outstanding Challenges." *Current Opinion in Solid State and Materials Science*, vol. 22, no. 3, June 2018, pp. 75-99, doi:10.1016/j.cossms.2018.05.002. Accessed 26 Feb. 2019.

6. Chahine, Gilbert, et al. "The Design and Production of Ti-6Al-4V ELI Customized Dental Implants." *JOM*, vol. 60, no. 11, 13 Nov. 2008, pp. 50-55, doi:10.1007/s11837-008-0148-2. Accessed 26 Feb. 2019.

7. Murr, L. E., et al. "Next-Generation Biomedical Implants Using Additive Manufacturing of Complex, Cellular and Functional Mesh Arrays." *Philosophical Transactions of the*

Royal Society A: Mathematical, Physical and Engineering Sciences, vol. 368, no. 1917, 28 Apr. 2010, pp. 368-404, doi:10.1098/rsta.2010.0010. Accessed 25 Feb. 2019.

8. Wang, Di, et al. "Study on the Designing Rules and Processability of Porous Structure Based on Selective Laser Melting (SLM)." *Journal of Materials Processing Technology*, vol. 213, no. 10, Oct. 2013, pp. 1734-42, doi:10.1016/j.jmatprotec.2013.05.001. Accessed 26 Feb. 2019.

9. Harrysson, Ola L. A., et al. "Direct Metal Fabrication of Titanium Implants with Tailored Materials and Mechanical Properties Using Electron Beam Melting Technology." *Materials Science and Engineering: C*, vol. 28, no. 3, 1 Apr. 2008, pp. 366-73, doi:10.1016/j.msec.2007.04.022. Accessed 21 Feb. 2019.

10. Su, Xu-bin, et al. "Development of Porous Medical Implant Scaffolds via Laser Additive Manufacturing." *Transactions of Nonferrous Metals Society of China*, vol. 22, Oct. 2012, pp. s181-s187, doi:10.1016/S1003-6326(12)61706-3. Accessed 21 Feb. 2019.

11. Souza, José, et al. "Micromechanical Analysis of the Effective Properties of Lattice Structures in Additive Manufacturing." *Additive Manufacturing*, vol. 23, Oct. 2018, pp. 53-69, doi:10.1016/j.addma.2018.07.007. Accessed 26 Feb. 2019.

12. Rakish Shrestha, Amanda Sterling, Brandon Lessel, Nam Phan, Mohammad Reza Vaziri Sereshk, Nima Shamsaei "Mechanical Behavior of Additively Manufactured 17-4 PH Stainless Steel Schoen Gyroid Lattice Structure", *Proceeding of the 29th Annual International Solid Freeform Fabrication Symposium - An Additive Manufacturing Conference*, Austin, TX, August 13-15, 2018.

13. Chen, Qizhi, and George A. Thouas. "Design Optimization of Supports for Overhanging Structures in Aluminum and Titanium Alloys by Selective Laser Melting." *Materials Science and Engineering: R: Reports*, vol. 87, Jan. 2015, pp. 1-57, doi:10.1016/j.mser.2014.10.001. Accessed 25 Feb. 2019.

14. Hibbeler, R. C. Mechanics of Materials. Prentice Hall, 2014.

15. Wehmöller, Michael, et al. "Implant Design and Production—a New Approach by Selective Laser Melting." *International Congress Series*, vol. 1281, May 2005, pp. 690-95, doi:10.1016/j.ics.2005.03.155. Accessed 21 Feb. 2019.